JOURNAL OF MATERIALS SCIENCE 25 (1990) 2827–2834

The limit of non-stoichiometry in silicon carbide

DUNBAR P. BIRNIE III*, W. DAVID KINGERY*
Department of Materials Science and Engineering, Massachusetts Institute of Technology, Cambridge, Massachusetts 02139, USA

The extent of the silicon carbide single-phase stability field has been investigated. Samples were equilibrated at 2400° C by coarsening of fine-grain silicon carbide powder. The lattice parameter, density, and the silicon-to-carbon ratio were measured on silicon- and carbon-saturated samples. These two compositions were not distinguishable at a level of better than one part in one thousand by their molecular weights per mole of crystal sites; no native point defects measurably respond to the difference in silicon activity. The accuracy of the lattice parameter and density measurements require that the free energies of defect pair formation be larger than about 3 eV. This applies to antisite pairs, Frenkel pairs *and* Schottky pairs. It is concluded that silicon carbide is largely stoichiometric. The crystal chemistry must be dominated by electrons, holes and impurities.

1. Introduction

Silicon carbide is a useful high-temperature structural ceramic. It can be sintered to near theoretical density with the simultaneous addition of boron and graphite. This observation is interesting because the sintering process is often closely linked to simple point defects and diffusion. The boron and carbon may be adjusting the defect concentrations to facilitate the densification process; boron is an acceptor impurity and graphite may define the carbon activity. In spite of the importance of point defects in processing, little is known about native point-defect formation in this system.

This paper presents an effort to manipulate the defects in silicon carbide for the purpose of identifying the majority species. The silicon activity is used to influence the defect concentrations. First, literature pertaining to non-stoichiometry and point defects is reviewed; past work related to this question has helped to focus the present investigation. Next, the experimental procedures used are described and the results given. Finally, a discussion of the results allows some definite conclusions to be made about defect formation in this system.

2. Literature review

The main body of literature motivating this study is the variety of reports of significant deviations from a stoichiometric silicon-to-carbon ratio. Direct chemical analyses of both beta-3C and alpha-6H single crystals by two different laboratories have reported the crystals to be silicon-rich [1, 2], while another report calls silicon carbide stoichiometric [3], as shown in Table I. A sintering study gave an indication that silicon carbide is silicon-rich by up to 5% [4]. Chemical analyses of NBS reference materials may also indicate that silicon carbide is slightly silicon-rich, but the numbers can only be estimated due to insufficient information [7]. One group [6, 8] has done a comparison of the stoichiometry of different silicon carbide polytypes using electron microprobe analysis, and reports a linear trend in the non-stoichiometry with the fraction of hexagonality. A backscattering study has also shown a silicon excess [5].

Thus, both direct chemical analysis and other methods seem to favour the interpretation that silicon carbide has an excess of silicon dissolved in the lattice. In contrast, the reported lattice parameters are all in general agreement; the fact that there are not large differences might be taken as evidence that silicon carbide is stoichiometric [9–21].

The density of single-crystal silicon carbide has been measured by several workers. Conwicke [20] found densities of the cubic polytype between 3.2105 and 3.2122 g cm^{-3} at 23° C for pure single crystals grown by chemical vapour diffusion. It seemed that the density was a function of the location of the crystal on the substrate, suggesting non-equilibrium deposition. He also measured some silicon-solution-grown crystals, getting densities between 3.2117 and 3.2119 g cm^{-3}. On 6H polytype crystals of an unknown genesis, densities of 3.2125 and 3.2123 g cm^{-3} were reported.

These densities are similar to the calculated crystallographic densities for 3C and 6H polytypes. Using the Gol'dshmidt *et al.* [12] data yields densities of 3.2142 and 3.2147 g cm^{-3} for 3C and 6H polytypes, respectively, while Conwicke calculated a crystallographic density of 3.2129 g cm^{-3}. The difference between the observed and calculated densities may not be significant. The actual variation in the density between the samples that he measured is relatively small, less than one-tenth of one per cent. These data also seem to indicate that silicon carbide may be relatively stoichiometric.

Some densities measured using a temperature gradient method were consistently lower [6] than

Present address: University of Arizona, Department of Materials Science and Engineering, Tucson, Arizona 85721, USA.

0022–2461/90 $03.00 + .12

TABLE I Reported non-stoichiometry in silicon carbide crystals

Method	Reference	Silicon-to-carbon ratio	Polytype
Chemical analysis	[1]	1.032	6H
	[2]	1.022 ± 0.016	6H
	[1]	1.049	3C
	[3]	1.000 ± 0.005	?
	[4]	1.05	3C
Helium backscattering	[5]	1.04	3C
Electron microprobe comparison with 6H	[2]	1.030	3C
	[6]	1.046	3C
	[6]	1.029	8H
	[6]	1.022	6H
	[6]	1.012	15R
	[6]	1.008	27R
	[6]	1.001	4H

theoretical. This was taken as evidence for large concentrations of vacancy-type defects. The crystals were grown by the Lely method at 2600° C, like many crystals grown by other workers. The disagreement with other studies is unclear.

Self-diffusion of silicon and carbon in silicon carbide has been measured for single-crystal and polycrystalline samples at different dopant levels [22–27]. Both the carbon and silicon diffusivities have high activation energies and high pre-exponential terms, suggesting vacancy diffusion mechanisms [22–24, 26]. The high activation energies combine energies of vacancy formation and vacancy migration.

The large reported deviations from stoichiometry cannot be derived from concentrations of either silicon interstitials or carbon vacancies. If either of these defects were present in percentage-level amounts then the diffusion behaviour would be markedly different. Silicon interstitials might have caused faster silicon diffusion and carbon vacancies would have forced a lower diffusion activation energy. This would suggest the remaining simple point-defect possibility: silicon antisite defects. This inference of silicon antisites led to the proposal of an interacting defect diffusion model for silicon self-diffusion in silicon carbide [28]. The model predicted these defects to be at levels near one per cent, in accord with a theoretical model that predicted antisite defects should be easy to form in silicon carbide (about 0.9 eV per pair) [29].

In summary, the presently available literature gives no consistent, quantitative picture of native point-defect formation in silicon carbide. The indication, primarily from chemical analysis, is that silicon carbide is somewhat silicon-rich.

3. Experimental procedure

First, the equilibration procedure for the samples to be measured is outlined. Then, each experimental technique used to evaluate the material is described. Samples were equilibrated at high temperature exposed to different silicon activities to create different defect populations. These samples were examined with X-ray diffraction, bulk density measurement and chemical analysis.

The equilibration of samples was achieved by high-temperature anneals of very fine-grain silicon carbide powder. Powder was chosen as the starting material to ensure equilibration. During the anneals appreciable coarsening occurred, such that essentially all (ca. 99.99%) of the crystalline material was formed at the temperature of annealing. This prevented non-equilibrium grown-in point-defect concentrations that otherwise might have been present. Also, the starting grain size was much smaller than the anticipated diffusion lengths for carbon and silicon in the lattice, also ensuring equilibration.

The starting powder was a commercially available 3C-silicon carbide with an average grain size of about 0.25 μm (Beta-rundum Ultra-fine, Ibiden Co. Ltd, Ogaki, Japan). It was mixed with a second phase (silicon or carbon) to establish a known thermodynamic reference for equilibration. Both carbon- and silicon-saturated compositions were created, one by adding powdered graphite (spectroscopic grade), and one by adding chunks of silicon (6N metals). By comparing these most extreme compositions, the greatest difference in defect concentration should be found. Large amounts of second phase were added to ensure that the equilibrium activities were indeed achieved. About 15% of the second phase was added in each case. Each two-phase mixture was placed in a graphite crucible with a well-fitting screw cap. For the silicon phase-boundary equilibration it was felt that the relatively high vapour pressure of silicon and the large fraction present would dominate the environment in the crucible. This can be justified by showing that all graphite surfaces grow protective layers of silicon carbide which contain the silicon activity at unity inside.

The equilibration temperature was chosen as high as reasonably possible to maximize the concentration of defects present. The temperature used was 2400° C. Much higher temperatures would have caused silicon to evaporate, making it harder to fix the silicon activity during the whole anneal. The samples were heated in a carbon tube resistance furnace controlled manually, giving an accuracy of about ± 20° C. The temperature was measured with an optical pyrometer. Both samples were annealed for two hours and then removed from the hot zone in about two seconds with a graphite push-rod.

To prevent loss of defects during quenching, some optimum quenching rate must be achieved [30]. Using a 10 μm grain size as the required resolution, and the carbon diffusivity (the faster species) as a worst case, the required cooling rate from 2400° C is about 2.6° C sec^{-1}. Using the thermal properties of silicon carbide, the radiative heat transfer is Newtonian (surface-limited). For a 1 cm radius crucible the calculated cooling rate is about 40.0° C sec^{-1}, significantly faster than required by point-defect kinetics. Both samples had grain sizes larger than this 10 μm thickness. This increases the confidence level of the quenching procedure.

After equilibration the excess second phases were removed. This allowed the chemical analysis and the density measurement to be done accurately. Each polycrystalline mass was removed from its crucible

and pulverized using a small hammer. An ASTM standard sieve was used to size the powder during crushing. The powder was subdivided down to a size of 125 μm or smaller. This crushing process also served to expose second phases entrained during growth. The crystals are more likely to break at the interfaces. These uniform powders were heated in air for 24 h at 700° C to remove the remaining graphite constituent. The removal of the graphite was evidenced by the change in colour of the graphite-rich sample from black to greenish. The silicon-rich sample stayed black due to the remaining elemental silicon. The final step was an acid wash using a mixture of HF, nitric acid and acetic acid in the ratio 3 : 5 : 3 to remove silicon, silica, and metals. This acid combination reacts very violently with silicon; it can be diluted with water to reduce its reactivity. The solution was used neat, adding the powder very slowly to keep the reaction under control. Care should be used when performing this treatment. The acid wash treatment was done on a Teflon filter with a 10 μm hole size; the apparatus was similar to normal water-pump aspirated filtration apparatus, except that a liquid trap was used in-line to prevent loss of acid. Thus, the final grain size could range from 10 to 125 μm, though the predominant fraction was near the larger end.

The lattice parameters of these samples were evaluated by Debye–Scherrer X-ray diffraction. Films were read using a standard Debye–Scherrer film reader (limit of precision = 0.005 cm or 0.1°). The film was allowed to warm up with the film reader for at least half an hour before affixing the film and making any measurements (it gets warmer and expands when the light is on). The film was aligned vertically so that the centre of the film was exactly under the crosshairs of the sliding film viewer. The film centre for our camera geometry was calculated to be 1.40 cm from the linear shadow on the film. This shadow is made by the inside lip on the back face of the camera. This film centre height was measured near both holes in the film and marked. These two points were used to align the whole strip of film.

Each diffraction line was located with the crosshairs in the magnifying lens of the film reader. Care was taken to prevent parallax errors while reading lines on opposite ends of the film. A scratch on the top surface of the magnifying lens was lined up with the crosshairs (on the bottom surface of the lens). These two were then lined up with the centre of the diffraction line. By lining up these three features, each diffraction line was read most accurately. The lattice parameters were calculated by least-squares fitting. The function that was minimized was the sum of the square of the difference between observed and predicted diffraction line location. All diffraction lines were weighted equally. Thus the lattice parameters were found at the condition where the observed pattern and the calculated pattern were in best agreement.

The computer program corrected for film shrinkage and off-centre sample location. The X-direction centre variable automatically corrects for sample absorption [31]; sample absorption is not significant for low atomic mass elements like silicon and carbon. A correction for non-linear film shrinkage was also tried, but did not increase the accuracy of the results. Four variables were used to describe the camera geometry:

(i) the film location of the collimator;
(ii) the film location of the beam stop; and
(iii, iv) the x and y deviation of the sample from the camera centre.

Additional variables were used depending on the number of parameters needed to describe the crystal lattice. The 3C polytype needed only one more parameter, while the hexagonal polytype required two parameters. The accuracy of the fitting was evaluated at two different levels. First, the r.m.s. line deviation was calculated at the condition of best fit. This gave an estimate of the typical average error per line during the measurement of the film. Second, this average error per line was used at the highest angle reflection to find the expected error in the interplanar spacing [31]:

$$\Delta d/d = -\overline{\Delta\theta} \cot \theta \quad (1)$$

where θ is half the angle from the beam stop to the diffraction line. The highest-angle diffraction line is the most accurate. This inferred error was used as the reported accuracy of the fitted lattice parameters.

The powder densities were measured in a density gradient column. The density gradient was created by mixing different density liquids together. The two endpoint liquids chosen were di-iodomethane and dibromomethane; they span the desired density range. They both have viscosities similar to water at room temperature and are transparent. The density column is built by applying a vacuum to the top of a burette and drawing in a varying linear mixture of the two endpoint liquids. This linear mixture is created with a two-beaker siphon set-up; the liquid is withdrawn from the beaker with the initially lower density. The rate of liquid withdrawal must be slow enough to have the liquid levels remain equal [32]. Before being introduced to the density column, each powder was immersed in the less dense liquid and vacuum-boiled to remove any air bubbles. They were then inserted into the density column and given 24 h to float to their equilibrium level, where the liquid density is exactly equal to the sample density (larger particles settle much faster than this). The particle distribution was measured photographically. An optical-quality single crystal of calcium fluoride was used to standardize the density as a function of location, and the two endpoint liquids were used to calibrate the density gradient. The crystal was produced commercially for infrared transmission windows. Its crystallographic density was calculated using the room-temperature lattice parameter [33].

Chemical analyses on the powders were done at the analytical laboratories of Norton Co. (Worcester, Massachusetts). Total carbon and silicon, and free carbon, silicon, and silica were measured. Their procedure conformed to the NBS procedure [7]. These numbers were used to calculate the stoichiometry of the silicon carbide. It was assumed, due to the extensive chemical pre-treatment, that no other phases would be present.

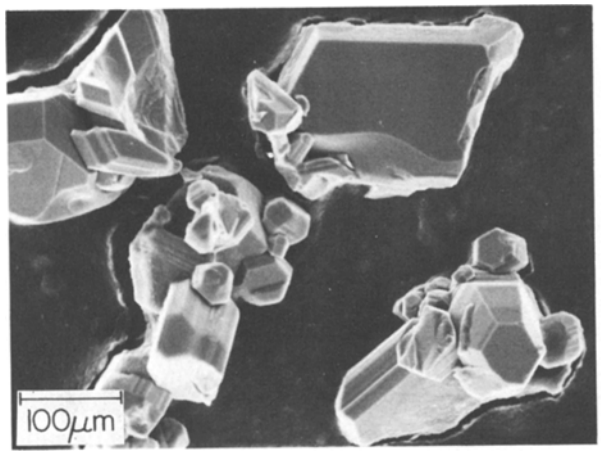

Figure 1 SEM micrograph of silicon carbide grains after equilibration in the silicon-rich environment. The grains were predominantly beta (3C) cubic silicon carbide.

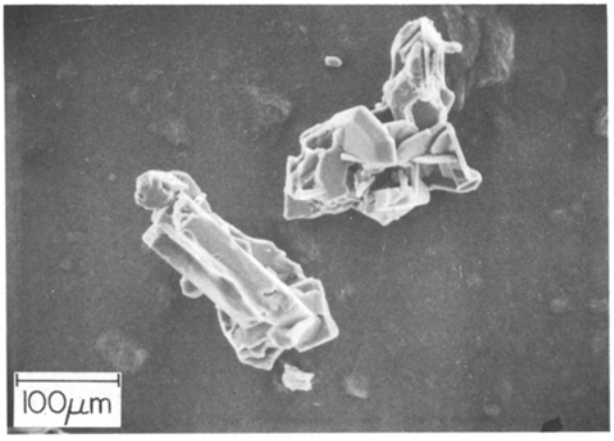

Figure 2 SEM micrograph of silicon carbide grains after equilibration in the carbon-rich environment. The grains were predominantly alpha (6H) hexagonal silicon carbide. Note the much more platy appearance.

4. Results

The two-phase boundary compositions grew to be different polytypes. The silicon-equilibrated sample grew as the 3C polytype, corroborating observations made by many other workers. The carbon-equilibrated sample grew as the 6H polytype, though some lines in the diffraction pattern suggested the presence of other polytypes at low levels. Fig. 1 shows the morphology of the silicon-equilibrated samples as seen by SEM. Fig. 2 shows the morphology of the carbon-equilibrated sample. Both samples are highly twinned. The silicon-equilibrated sample was noticeably different from the carbon-equilibrated, evidencing the different polytypes that were obtained.

Table II has the lattice parameter results from the fitting program. It was found that the use of the X-direction sample off-centre correction was more important than the Y-direction variable. Moving the sample in the X direction causes the rings to appear smaller or larger, while moving in the Y direction moves the opposite sides of the diffraction line in opposite directions; this type of correction can be accommodated somewhat by different collimator and beam-stop locations. Note that the addition of the X-direction freedom (going from Case (a) to Case (b) in Table II) improves the average diffraction line error, but there is little improvement from Case (b) to Case (c). Also, the values of the best-fit lattice parameters change only insignificantly by the inclusion of the Y-direction correction. The r.m.s. line errors for all cases are smaller than the precision of the film reader, indicating good fits. The lattice parameter accuracies in this table have been calculated using Equation 1 at the highest-angle diffraction line.

Table III has the diffraction line locations as measured and the observed and calculated interplanar spacings for each of the reflections. The line locations in Table III use only the X-direction correction (Case (b) above). Only the diffraction lines that were unambiguously identifiable were used for fitting and included in the table.

The calibration data for the density column are given in Table IV. These numbers were used to calculate the density values for the two equilibrated samples. These are reported in Table V. They exhibit slightly different densities from each other. The value for the difference between their densities is more accurate than either of the absolute densities. The errors in the density gradient or the density standard value cancel when comparing samples.

The silicon-rich sample was very narrowly distributed in the density column, indicating a high level of uniformity. The carbon-rich sample was spread over several millilitres. Grains of the carbon-rich sample were examined with optical microscopy using high refractive index liquid immersion. Some of the grains had barely visible inclusions. The spread in the density for this sample is probably due to small amounts of second phase being present. All possible second

TABLE II Lattice parameters from fitting procedure: (a) both ΔX and ΔY camera centre deviations fixed to zero, (b) only ΔY camera centre deviation fixed to zero, (c) both ΔX and ΔY free to vary during fitting

Case	ΔX (cm)	ΔY (cm)	a (nm)	c (nm)	r.m.s. line error (cm)
Carbon-equilibrated sample (predominant polytype: 6H)					
(a)	*	*	0.308105 ± 0.000027	1.51179 ± 0.00014	0.0049
(b)	0.0060	*	0.308146 ± 0.000021	1.51207 ± 0.00010	0.0038
(c)	0.0044	−0.0011	0.308141 ± 0.000021	1.51203 ± 0.00010	0.0038
Silicon-equilibrated sample (predominant polytype: 3C)					
(a)	*	*	0.435846 ± 0.000043		0.0042
(b)	0.0067	*	0.435964 ± 0.000027		0.0026
(c)	0.0061	−0.0004	0.435960 ± 0.000027		0.0026

*These values were constrained to be zero during the fitting for these cases.

TABLE III Observed and calculated diffraction patterns

hkl	D_{calc} (nm)	D_{obsv} (nm)	Location (cm)	Wavelength*
(a) Carbon-equilibrated sample. Data using fitting results from Table II, Case (b). Miller indices referenced to hexagonal unit cell (i index omitted).				
10 9	0.142177	0.14210	41.305	α_2
10 9	0.142177	0.14210	41.285	α_1
10 7	0.167899	0.16791	39.925	α
10 7	0.167899	0.16800	39.250	β
10 5	0.200094	0.19997	38.800	α
10 3	0.235844	0.2359	37.940	α
10 3	0.235844	0.2358	37.500	β
10 1	0.262801	0.2630	37.460	α
10 1	0.262801	0.2630	37.070	β
10 1	0.262801	0.2631	29.885	β
10 1	0.262801	0.2628	29.490	α
10 3	0.235844	0.2359	29.455	β
10 3	0.235844	0.2358	29.010	α
10 5	0.200094	0.20001	28.155	α
10 7	0.167899	0.16763	27.690	β
10 7	0.167899	0.16794	27.030	α
10 9	0.142177	0.14206	26.515	β
10 9	0.142177	0.14212	25.670	α_1
10 9	0.142177	0.14212	25.650	α_2
20 1	0.132915	0.13292	25.005	α
20 3	0.128988	0.12896	24.680	α
20 7	0.113520	0.113540	23.075	α_1
20 7	0.113520	0.113554	23.045	α_2
20 8	0.109005	0.108986	22.440	α_1
20 8	0.109005	0.108992	22.405	α_2
20 9	0.104487	0.104480	21.695	α_1
20 9	0.104487	0.104487	21.655	α_2
12 1	0.100641	0.100649	20.930	α_1
12 1	0.100641	0.100642	20.880	α_2
10 14	0.100116	0.100114	20.810	α_1
10 14	0.100116	0.100112	20.760	α_2
12 3	0.098903	0.098907	20.525	α_1
12 3	0.098903	0.098899	20.470	α_2
11 12	0.097540	0.097546	20.175	α_1
11 12	0.097540	0.097555	20.120	α_2
12 4	0.097455	0.097454	20.150	α_1
12 4	0.097455	0.097500	20.105	α_2
10 15	0.094301	0.094299	19.165	α_1
10 15	0.094301	0.094326	19.100	α_2
12 7	0.091392	0.091388	17.840	α_1
12 7	0.091392	0.091391	17.720	α_2
12 7	0.091392	0.091382	13.240	α_2
12 7	0.091392	0.091387	13.115	α_1
10 15	0.094301	0.094298	11.865	α_2
10 15	0.094301	0.094298	11.790	α_1
12 4	0.097455	0.097445	10.865	α_2
12 4	0.097455	0.097452	10.805	α_1
11 12	0.097540	0.097554	10.835	α_2
11 12	0.097540	0.097526	10.785	α_1
12 3	0.098903	0.098898	10.485	α_2
12 3	0.098903	0.098906	10.430	α_1
10 14	0.100116	0.100111	10.195	α_2
10 14	0.100116	0.100112	10.145	α_1
12 1	0.100641	0.100663	10.070	α_2
12 1	0.100641	0.100648	10.025	α_1
20 9	0.104487	0.104486	9.300	α_2
20 9	0.104487	0.104478	9.260	α_1
20 8	0.109005	0.109055	8.540	α_2
20 8	0.109005	0.109051	8.505	α_1
(b) Silicon-equilibrated sample. Data using fitting results from Table II, Case (b). Miller indices referenced to cubic unit cell.				
31 1	0.131448	0.13142	41.330	α_2
31 1	0.131448	0.13151	41.300	α_1
22 2	0.125852	0.12585	40.745	β
31 1	0.131448	0.13145	40.340	β
22 0	0.154137	0.15413	39.840	α_2
22 0	0.154137	0.15417	39.820	α_1
22 0	0.154137	0.15403	39.075	β
20 0	0.217982	0.2179	37.575	α
20 0	0.217982	0.2179	37.090	β
11 1	0.251704	0.2517	36.890	α
11 1	0.251704	0.2520	36.475	β
11 1	0.251704	0.2515	28.950	β
11 1	0.251704	0.2518	28.545	α
20 0	0.217982	0.2180	28.345	β
20 0	0.217982	0.2178	27.855	α
22 0	0.154137	0.15420	26.365	β
22 0	0.154137	0.15412	25.610	α_1
22 0	0.154137	0.15417	25.595	α_2
31 1	0.131448	0.13148	25.095	β
22 2	0.125852	0.12582	24.685	β
31 1	0.131448	0.13141	24.125	α_1
31 1	0.131448	0.13145	24.105	α_2
22 2	0.125852	0.12585	23.645	α_1
22 2	0.125852	0.12586	23.620	α_2
40 0	0.108991	0.10902	23.100	β
33 1	0.100017	0.100025	21.880	β
40 0	0.108991	0.108977	21.670	α_1
40 0	0.108991	0.108950	21.630	α_2
33 1	0.100017	0.100024	20.020	α_1
33 1	0.100017	0.100024	19.970	α_2
42 2	0.088991	0.088995	19.585	β
42 0	0.097485	0.097472	19.385	α_1
42 0	0.097485	0.097482	19.330	α_2
33 3	0.083901	0.083911	17.710	β
33 3	0.083901	0.083891	11.710	β
42 0	0.097485	0.097480	10.080	α_2
42 0	0.097485	0.097489	10.020	α_1
42 2	0.088991	0.088993	9.825	β
33 1	0.100017	0.100022	9.440	α_2
33 1	0.100017	0.100022	9.390	α_1
42 0	0.097485	0.097503	7.950	β
40 0	0.108991	0.108979	7.775	α_2
40 0	0.108991	0.108974	7.740	α_1
33 1	0.100017	0.100021	7.530	β
40 0	0.108991	0.10902	6.310	β

*α = 0.179026 nm, α_1 = 1.788965 nm, α_2 = 0.179285 nm, β = 0.162079 nm.

phases have lower density. Therefore, the denser edge of the density distribution was used as representative of perfect crystals.

The lattice parameters were used to calculate the volume occupied per unit cell. These values, given in Table V, are normalized to the number of silicon carbide molecules in the unit cell (6H has six and 3C has four). The two cell volumes are not significantly different from each other.

The density and cell volume values were used to

TABLE IV Density gradient column calibration information

Pure liquid densities ($g\,cm^{-3}$) at room temperature:
- Di-iodomethane 3.3254
- Dibromomethane 2.4956

Endpoint liquid densities:
- Top of column density = 3.1179 (45 ml) di-iodomethane + 15 ml dibromomethane)
- Bottom of column density = 3.3254 (60 ml di-iodomethane)

Calculated density gradient = 1.729×10^{-3} ($g\,cm^{-3}\,ml^{-1}$)

Calcium fluoride standard (IR window grade single crystal, no flaws):
- Density = 3.1810 (crystallographic)
- Location in column = 53.8 ml

Temperature of column = 26.4 ± 0.1° C

TABLE V Sample densities

Property	Phase boundary of equilibration	
	Carbon	Silicon
Predominant polytype	6H	3C
Location in column (ml)	69.0 ± 0.4	70.3 ± 0.2
Density ($g cm^{-3}$)*	3.2073 ± 0.0022	3.2095 ± 0.0018
Unit cell volume (nm^3)	0.0207235 ± 0.0000041	0.0207153 ± 0.0000038
Molecular weight ($g mol^{-1}$)	40.034 ± 0.03	40.045 ± 0.03

*Errors include an allowance for up to 5% deviation in the linear density gradient.

calculate the weight, in grams, of the atoms occupying one mole of silicon and carbon sites. This molecular weight is given at the bottom of Table V. The molecular weights for the carbon- and silicon-saturated compositions are not significantly different from each other. This similarity occurs in spite of the slightly different densities. The lattice parameters showed a trend in a direction to counteract the difference in the densities. The molecular weights appear to be different from the ideal value of 40.097. This may be due to some small error in the density standard, but the *comparison* between the two samples is still valid: there is no significant difference.

The chemical analysis for the two powders is given in Table VI. The absence of large concentrations of any second phase is conspicuous. This validates the chemical cleaning procedure for removing second-phase material. Only the total carbon and free carbon were measured repeatedly.

The stoichiometry of the two samples was calculated as the ratio of the measured silicon in silicon carbide to the measured carbon in silicon carbide. This is reported as the last entry of Table VI. Two types of error bar are given. The first uses only the error from the total carbon measurements. The second set of error bars includes the uncertainty due to the fact that the analyses do not add up to 100%. In contrast to most previous literature reports, both samples show a silicon-to-carbon ratio of unity, at an accuracy level of only 1%. The stoichiometry cannot be quoted more accurately than this.

In summary, the chief measure of the difference between the two samples must be the molecular weight. This cancels any difference in molar volume due to polytype variations. These values for the two samples are not significantly different from each other, even considering only the relative error contributions for the difference in density. The comparison is more accurate than one part in 1000, better than the present chemical analysis by a factor of ten.

TABLE VI Chemical analysis results (wt %)

Component	Equilibration	
	Carbon	Silicon
Total carbon	29.89 ± 0.22	29.66 ± 0.04
Si in SiC	69.72	69.35
Free carbon	0.03	0.01
Free silicon	0.02	0.02
Free silica	0.10	0.08
Total weight	99.73 ± 0.22	99.12 ± 0.04
SiC	0.999 ± 0.007 (±0.010)*	1.000 ± 0.001 (± 0.010)*

*For explanation see text.

5. Discussion

There is no measurable difference in the molecular weight per mole of sites as shown in Table V. Table VII shows a list of simple neutral point defects that could be present, their silicon partial pressure exponent, and their molar weight with respect to the perfect lattice. All of these defects respond to the activity difference during annealing, and they each have a different mass to their host site. Therefore, if any one of these neutral point defects dominated the crystal chemistry, then the mass would be different across the single-phase field. Since there is no observable difference in molecular weight, then all of these defects must be below some threshold concentration. The ratio of silicon activities for the two anneals will define this detectability limit.

Using thermodynamic data for the formation of silicon carbide from the elements [34], the activity of silicon at the opposite phase boundaries can be calculated. At 2400° C the standard state for silicon is the liquid, therefore the formation reaction can be written

$$C(gr) + Si(l) = SiC(s, \alpha) \quad (2)$$

The free energy of formation for this reaction at 2400° C is $-5.21 kcal mol^{-1}$ ($-21.81 kJ mol^{-1}$). At equilibrium the following equation is satisfied:

$$\Delta G^f = -RT \ln (a_{SiC}/a_C a_{Si}) \quad (3)$$

where a represents activity. At the carbon phase boundary ($a_{SiC} = 1$ and $a_C = 1$) the activity of silicon can be determined by

$$\Delta G^f = RT \ln (a_{Si}) \quad (4)$$

At 2400° C the activity of silicon at the carbon phase boundary is 0.37. At the silicon-rich phase boundary the silicon activity is by definition unity. The ratio of defect concentrations in the opposite phase boundary compositions at 2400° C is simply the ratio of these activities taken to the appropriate power from Table VII. This concentration ratio is listed as the last entry of the table.

If any one of these point defects were significant then the molecular weight would be a simple function of the silicon activity. Since the molecular weight does

TABLE VII Silicon activity relationships for simple point defects

Neutral point defect	Silicon partial pressure exponent	Defect molar weight with respect to lattice ($g\,mol^{-1}$)	Concentration ratio at opposite phase boundaries [ ](C)/[ ](Si)
V_C	1	−12	0.37
V_{Si}	−1	−28	2.7
C_{Si}	−2	−16	7.1
Si_C	2	16	0.14

not change measurably across the phase field (the change is smaller than 0.03 g relative to 40 g), then none of these defects is present in large concentration. The experimentally determined maximum defect concentration change due to equilibration is simply this weight-change limit (0.03 g) divided by the molar weight of the defect. This value is given in Table VIII. Using this maximum concentration difference and the ratio of concentrations given before in Table VII, each of the maximum defect concentrations can be found at both phase boundaries. These are given last in Table VIII.

These concentrations can be used to find a limit on the free energies of defect formation. For the Schottky pair reaction the equilibrium constant is simply the product of the vacancy concentrations at one of the phase boundaries, and the antisite pair formation reaction is the product of the antisite defect concentrations. Both of these limiting equilibrium constants are given in Table VIII. These equilibrium constants define limits for the free energy of these reactions. The Schottky reaction must have a free energy of formation greater than 2.9 eV and the antisite pair reaction must have a formation energy greater than 3.2 eV. These are lower limits on the possible pair formation energies. Any lower energy would have allowed some point defect to have been sensed through a change in molar weight. These are also rather pessimistic lower limits for the formation energy; it is unlikely that *both* defect concentrations were lurking just below the detectability limit. Many of these maximum concentrations shown in Table VIII are lower than the intrinsic electron and hole concentrations that would be found at this temperature (about 0.002 to 0.003). Therefore, it is expected that the major intrinsic disorder will be electronic. The above two limiting pair formation energies cannot be directly compared with the room-temperature band gaps of the polytypes; for example, the band gap for the 6H polytype should decrease from its room-temperature value near 3 eV to a value below 2.5 eV at 2400° C.

TABLE VIII Limiting concentrations for simple point defects

Neutral point defect	Experimental limit for concentration difference at phase boundaries	Maximum defect concentration at phase boundary (mole fraction)	
		Silicon	Carbon
V_C	0.0025	0.0040	0.0015
V_{Si}	0.0011	0.00065	0.00175
Schottky product: maximum = 0.0000026			
C_{Si}	0.0019	0.00031	0.0022
Si_C	0.0019	0.0022	0.00031
Antisite defect product: maximum = 0.0000007			

The comparison of the silicon- and carbon-saturated compositions is based on the assumption that the different polytypes of silicon carbide are chemically very similar and that point-defect formation in the different lattices is also very similar. The slight variation in the c/a ratio as a function of percentage hexagonality has been factored out by using the molecular weight per mole of sites as the probe of the point-defect concentrations. The fact that there is no measurable difference between the different polytypes grown at silicon and carbon saturation shows that this assumption is a good one. The different polytypes may grow as a result of kinetic influences rather than thermodynamic driving forces.

The variety of previous stoichiometry measurements are inconsistent with the current findings. It is believed that the refractory nature of silicon carbide makes accurate chemical analysis a difficult procedure. Referring back to Table VI, it can be seen that careful chemical analysis is not necessarily mass-conservative. The samples reported here have up to 1% deficit in the reported total measured weight. This was also true of NBS standard reference material No. 112 [7]; the average of five laboratories, each measuring multiple samples, gave only 99.0% total mass. Consistently 1% of the mass of the starting material was lost in the process. This means that these measurements can have an absolute accuracy of only 1%.

In the present results, the stoichiometries, calculated ignoring the loss in mass, are numbers not significantly different from unity, even using the precision values. The literature-reported stoichiometries that extend to a level of about 5% silicon excess cannot be well explained.

Referring again back to Table I, half of the reports of non-stoichiometry come from electron microprobe comparison of different polytypes. It should be noted that each of these measurements is referenced to some crystal that has been analysed chemically. Therefore, only the differences between samples should be examined. The present measurements on equilibrated powders show that the chemistries of the different polytypes must be very similar. The differences reported by the electron microprobe technique are too large to be explained by grown-in defect concentrations. Some feature of the silicon carbide polytypes or of the microprobe technique must be responsible for the observed differences. Two features of the electron probe generation of X-rays in silicon carbide

may create problems. First, along with any change in composition (the area of the Si$K\alpha$ peak), there is a shift in the wavelength of the characteristic X-radiation [6]. This wavelength shift could lead to intensity differences [35]. Second, the change in band gap with polytype [36] indicates some change in the lattice bonding, and this may also change the relative X-ray yields. At present, all of the different methods for determining the silicon-to-carbon ratio seem uncertain. Standardization of the techniques is difficult because there is no clearly definable reference state to use as stoichiometric.

In conclusion, the present indirect defect measurements yield no difference between silicon- and carbon-saturated powders of silicon carbide. There is no observed difference between polytypes; each seems to be largely stoichiometric. The present work shows that any defect pair reaction must have a formation energy larger than about 3 eV. The most abundant native defects at high temperature will be electrons and holes.

If the silicon carbide lattice is nearly stoichiometric then the silicon diffusion cannot proceed by the motion of silicon antisite atoms, as was previously proposed [28]. The diffusion model required up to 1% of grown-in silicon antisite defects, but at 2400° C the equilibrium antisite defect concentration must be below 0.2%.

6. Conclusions

Several conclusions can be drawn from the present work. First, it was observed that the silicon- and carbon-saturated crystals exhibited different polytypes, in agreement with the bulk of the literature. The silicon-equilibrated sample had the 3C polytype and the carbon-equilibrated sample had the 6H polytype.

Second, the molecular weights of carbon- and silicon-saturated compositions were not measurably different at a level of better than one part in one thousand. This indicates that the crystal is largely stoichiometric. The accuracy of this measurement requires that all types of defect pair reaction must have free energies of formation greater than about 3 eV at 2400° C.

Next, chemical analysis was found not to be reliable for the evaluation of the silicon-to-carbon ratio in silicon carbide. The refractory nature of silicon carbide yields data with an overall accuracy of only about 1.0%.

Finally, the diffusion model developed to explain features of the literature data is not supported by the current results. The conclusion of relative stoichiometry contradicts its prediction of up to 1.0% levels of silicon antisite defects.

Acknowledgement

The authors are grateful for the support of United States Department of Energy (Contract No. DE-AC02-76ER02390).

References

1. P. T. B. SHAFFER, *Mater. Res. Bull.* **S4** (1969).
2. V. A. IL'IN *et al.*, *Inorg. Mater.* **16** (1980) 699.
3. W. F. KNIPPENBERG, *Philips Res. Repts.* **18** (1963) 161.
4. J. HOJO *et al.*, *J. Amer. Ceram. Soc. Commun.* **66** (1983) c114.
5. M. NAGATOMO, H. ISHIWARA and S. FURUKAWA, *Jpn J. Appl. Phys.* **18** (1979) 765.
6. N. D. SOROKIN *et al.*, *Sov. Phys. Cryst.* **28** (1983) 539.
7. National Bureau of Standards, Reference Materials SRM 112 (1912) and SRM 112b (1985).
8. Y. M. TAIROV and V. F. TSVETKOV, in "Crystal Growth and Characterization of Polytype Structures", edited by P. Krishna (Pergamon, Oxford, 1983) pp. 111–161.
9. R. F. ADAMSKY and K. M. MERZ, *Z. Krist.* **111** (1959) 350.
10. H. OTT, *Naturwissenschaften* **13** (1925) 644.
11. Y. TAJIMA and W. D. KINGERY, *J. Amer. Ceram. Soc. Commun.* **65** (1982) c27.
12. R. GOL'DSHMIDT *et al.*, *Sov. Phys. Cryst.* **27** (1982) 371.
13. D. LUNDQVIST, *Acta Chem. Scand.* **2** (1948) 177.
14. G. BORRMANN and H. SEYFARTH, *Z. Krist.* **86** (1933) 472.
15. A. TAYLOR and D. S. LAIDLER, *Br. J. Appl. Phys.* **1** (1950) 174.
16. A. TAYLOR and R. M. JONES, in "Silicon Carbide", edited by J. R. O'Connor and J. Smiltens (Pergamon, New York, 1960) pp. 147–154.
17. T. KAWAMURA, *J. Mineralogy* **4** (1965) 333.
18. P. T. B. SHAFFER, *Mater. Res. Bull.* **S4** (1969) 213.
19. G. A. SLACK and R. I. SCACE, *J. Chem. Phys.* **42** (1965) 805.
20. J. A. CONWICKE, PhD thesis, Massachusetts Institute of Technology (1969).
21. H. SUZUKI and T. HASE, *J. Amer. Ceram. Soc.* **63** (1980) 349.
22. R. N. GHOSTAGORE, ScD thesis, Massachusetts Insitute of Technology (1965).
23. R. N. GHOSHTAGORE and R. L. COBLE, *Phys. Rev.* **143** (1966) 623.
24. M. H. HON and R. F. DAVIS, *J. Mater. Sci.* **14** (1979) 2411.
25. M. H. HON, R. F. DAVIS and D. E. NEWBURY, *ibid.* **15** (1980) 2073.
26. J. D. HONG and R. F. DAVIS, *J. Amer. Ceram. Soc.* **63** (1980) 546.
27. J. D. HONG, R. F. DAVIS and D. E. NEWBURY, *J. Mater. Sci.* **16** (1981) 2485.
28. D. P. BIRNIE III, *Amer. Ceram. Soc. Commun.* **69** (1986) c33.
29. J. A. VAN VECHTEN, *J. Electrochem. Soc.* **122** (1975) 423.
30. D. P. BIRNIE III and W. D. KINGERY, *J. Mater. Sci.* **20** (1985) 2193.
31. B. D. CULLITY, "Elements of X-Ray Diffraction", 2nd Edn (Addison-Wesley, Reading, Massachusetts, 1978) p. 354.
32. G. OSTER and M. YAMAMOTO, *Chem. Rev.* **63** (1963) 257.
33. Joint Committee on Powder Diffraction Standards, Card No. 4-864, American Society for Testing and Materials Publication (Philadelphia, Pa., 1966).
34. Joint Army, Navy, Air Force (JANAF) Thermochemical Tables, edited by D. R. Stull and H. Prophet (National Bureau of Standards, Gaithersburg, 1971).
35. T. R. SWEATMAN and J. V. P. LONG, *J. Petrology* **10** (1969) 332.
36. W. J. CHOYKE and L. PATRICK, in Proceedings of 3rd International Conference on Silicon Carbide, Miami Beach, Florida (1973), (U. South Carolina Press, Columbia, 1973) pp. 261–283.

Received 9 February
and accepted 29 April 1987